Journal of Solid State Chemistry 182 (2009) 1792–1797

Contents lists available at ScienceDirect

Journal of Solid State Chemistry

journal homepage: www.elsevier.com/locate/jssc

# Disordered pyrochlore $CsMgInF_6$ at high pressures

Andrzej Grzechnik [a,*], Wolfgang Morgenroth [b], Karen Friese [a]

[a] *Departamento de Física de la Materia Condensada, Universidad del País Vasco, Bilbao, Spain*
[b] *Institut für Geowissenschaften, FE Mineralogie, Abt. Kristallographie, Universität Frankfurt, Germany*

ARTICLE INFO

*Article history:*
Received 19 February 2009
Received in revised form
13 April 2009
Accepted 22 April 2009
Available online 3 May 2009

*Keywords:*
Crystal structure
Fluoride pyrochlore
Order–disorder
High pressure

ABSTRACT

High pressure behaviour of disordered pyrochlore $CsMgInF_6$ ($Pnma$, $Z=4$) has been studied with powder and single-crystal X-ray diffraction to 8.0 and 6.94 GPa, respectively, in diamond anvil cells at room temperature. The material is structurally stable to at least 8.0 GPa with no ordering of the $In^{3+}$ and $Mg^{2+}$ cations. The $P$–$V$ data are fitted by a Birch–Murnaghan equation of state with the zero-pressure bulk modulus $B_0=33.4(3)$ GPa and the unit-cell volume at ambient pressure $V_0=603.2(4)$ Å$^3$ for the first pressure derivative of the bulk modulus $B'=4.00$. The major contribution to the bulk compressibility arises from the changes in the coordination sphere around the Cs atoms. The effect of hydrostatic pressure on the crystal structure of $CsMgInF_6$ is comparable to the effect of chemical pressure induced by the incorporation of ions of different sizes into the $A$ and $B$ sites in defect $AB^{2+}B'^{3+}F_6$ pyrochlores.

## 1. Introduction

Ideal pyrochlore ($Fd\bar{3}m$, $Z=8$) has a formula $A_2B_2X_6X'$($A=$ Na, Rb, Cs, Ca, Sr, Mg, etc.; $B=$ Nb, Ta, Ti, Fe, etc.; $X$ and $X'=$ O, F, or OH). The $A$ cations are coordinated by eight anions, while the $B$ cations are in an octahedral coordination. When a large cation, like $Cs^{1+}$, $Rb^{1+}$, $K^{1+}$, or $NH_4^{1+}$ is incorporated into one of the $A$ sites (the other remaining empty) in fluoride pyrochlore, a defect structure with a formula $AB^{2+}B'^{3+}F_6$ is obtained. The coordination numbers of the $Cs^{1+}$ and $Rb^{1+}$ cations vary from 12+6 to 18.[1] There is only one symmetrically independent $B$ site in the ideal cubic structure so that the two $B^{2+}$ and $B'^{3+}$ cations are perfectly disordered. Ordering of these cations leads to symmetry lowering and the ordered compounds crystallize in space groups which are in a group–subgroup relation to $Fd\bar{3}m$ [1] (Fig. 1). $CsMgInF_6$ is a remarkable representative of the $AB^{2+}B'^{3+}F_6$ family [2] as no ordering of the $Mg^{2+}$ and $In^{3+}$ cations occurs on the $B$ site, although its symmetry is orthorhombic ($Pnma$, $Z=4$). The compound is multiply twinned at ambient conditions, the twinning elements being a combination of the three- and four-fold rotation axes of the archetype cubic lattice.

In our previous work on $NaCdZn_2F_7$ and $NaCaMg_2F_7$ ($Fd\bar{3}m$, $Z=8$), in which the $Na^{1+}/Cd^{2+}$ and $Na^{1+}/Ca^{2+}$ cations are perfectly disordered on the $A$ site, we demonstrated that they are structurally stable at least to 9.0 and 6.5 GPa, respectively, with no indication either for ordering or for structural transformations [3]. In this work, we continue our interest in disordered fluoride pyrochlores and investigate the crystal structure of $CsMgInF_6$ ($Pnma$, $Z=4$) at different pressures and room temperature. Our main goal is to examine (dis)ordering of the $Mg^{2+}$ and $In^{3+}$ cations and structural distortions using X-ray powder and single-crystal diffraction.

## 2. Experimental

Single-crystal and powder samples of $CsMgInF_6$ investigated here have already been used in Ref. [2].

The ruby luminescence method [4] was used for pressure calibration and a 4:1 mixture of methanol and ethanol was used as a pressure medium during the powder and single-crystal measurements. The error in pressure determination is estimated to be 0.02 GPa.

High-pressure room-temperature X-ray powder diffraction studies were performed at the beamline D3 in HASYLAB (Hamburg, Germany). Finely ground samples were loaded into a DXR-6 (Diacell) diamond anvil cell for angle-dispersive powder X-ray diffraction measurements to 8.0 GPa with monochromatic radiation at 0.4 Å. The collimator slits were set to $50\times50$ μm. The diamond cell was optically aligned on the four-circle diffractometer. The data were collected on a marCCD165 detector. The images were integrated with the program FIT2D [5] to yield intensity versus $2\theta$ diagrams. A fluorite powder was added as an

---

* Corresponding author. Fax: +34 94 601 35 00.
*E-mail address:* andrzej.grzechnik@ehu.es (A. Grzechnik).

[1] Although the $A$ atoms are generally surrounded by 18 fluorine atoms, only in some of the defect pyrochlores all the fluorines are the $A$ nearest neighbours. In several other compounds, a part of the fluorines is closer to the $A$ atoms, leading to coordination spheres best described as 12+6, 14+4, 15+3, or 16+2 [1,2].

0022-4596/$ - see front matter © 2009 Elsevier Inc. All rights reserved.
doi:10.1016/j.jssc.2009.04.026

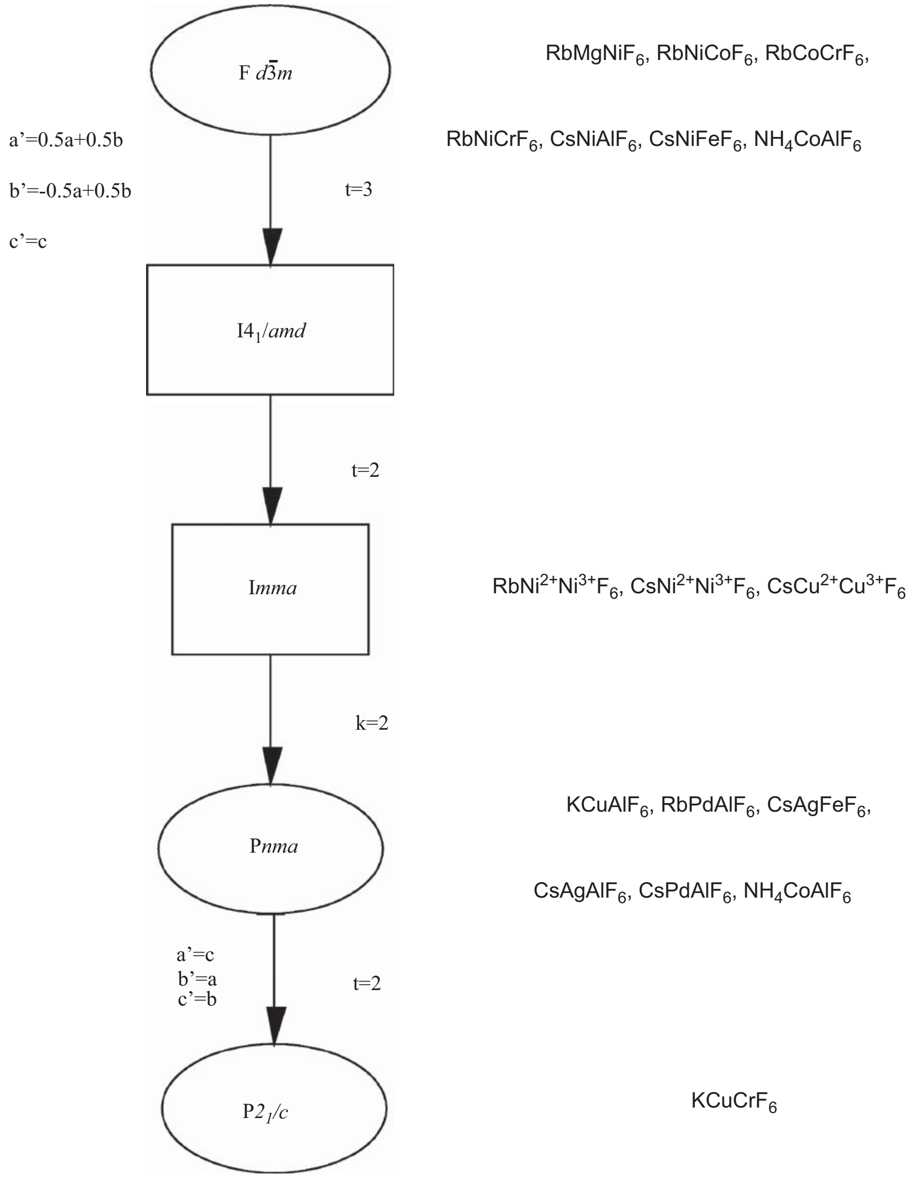

**Fig. 1.** Group–subgroup relationship for the $AB^{2+}B'^{3+}F_6$ pyrochlores with a few relevant examples included in Ref. [1].

internal standard for the $2\theta$ calibration at each pressure through the $CaF_2$ equation of state [6].

Single-crystal intensities were measured from a crystal with approximate dimensions $0.07 \times 0.04 \times 0.06$ mm at room temperature to 6.94 GPa in a diamond anvil cell of the Boehler-Almax type using a STOE diffractometer IPDS-2T (Mo$K\alpha$). A 250 μm hole was drilled into a stainless steel gasket preindented to a thickness of about 80 μm. The intensities were indexed and integrated using the STOE software [7]. Shaded areas of the images by the diamond anvil cell were masked prior to integration. The intensities were integrated simultaneously with three orientation matrices, corresponding to the crystal of $CsMgInF_6$ and to the two diamonds of the cell. The corrections for the effect of absorption by the diamond anvils and the crystal were made using the program Absorb [8] and the STOE software [7], respectively. Structural refinements were carried out with the program JANA2006 [9].[2]

## 3. Results and discussion

The lattice parameters and unit-cell volume of $CsMgInF_6$ (*Pnma*, $Z = 4$) at atmospheric pressure are $a = 7.5285(1)$ Å, $b = 7.5285(1)$ Å, $c = 10.6459(1)$ Å, and $V = 603.39(1)$ Å$^3$, respectively [2]. This metrics is not only tetragonal, but it also reflects the cubic lattice of the underlying ideal pyrochlore structure, $a = b \approx c/\sqrt{2}$. As a consequence, splitting of reflections indicating the symmetry reduction in X-ray powder diffraction diagrams is difficult to detect at atmospheric pressure. In addition, the reflections violating the extinction rules for the cubic face-centered lattice (or the tetragonal/orthorhombic body-centered lattice) and thus providing the conclusive indication for the symmetry lowering are extremely weak. However, our powder X-ray data collected at high pressures clearly demonstrate splitting of reflections due to either an anisotropic compressibility of the material or a pressure-induced phase transition (Fig. 2). All the changes in the patterns are reversible on decompression, although the reflections are slightly more broadened and thus worse resolved than before the compression.

---

[2] Further details of the crystallographic investigations can be obtained from the Fachinformationszentrum Karlsruhe, D-76344 Eggenstein-Leopoldshafen, Germany, on quoting the depository number CSD 420660.

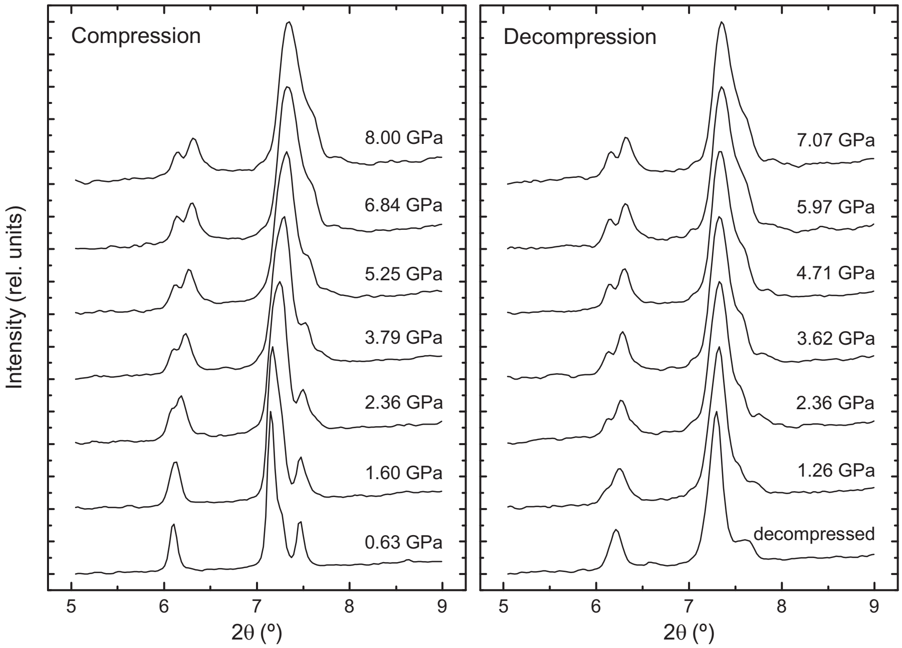

**Fig. 2.** X-ray powder diffraction diagrams in the $2\theta$ range from 5° to 9° as a function of pressure.

**Table 1**
Pressure dependence of lattice parameters and unit-cell volume.

| Pressure (GPa) | $a$ (Å) | $b$ (Å) | $c$ (Å) | $V$ (Å$^3$) |
|---|---|---|---|---|
| 0.0001 | 7.5285(1) | 7.5285(1) | 10.6459(1) | 603.4 |
| 1.08 | 7.435(3) | 7.489(3) | 10.491(4) | 584.1 |
| 2.32 | 7.332(3) | 7.467(4) | 10.368(4) | 567.6 |
| 3.39 | 7.240(4) | 7.432(4) | 10.289(4) | 553.6 |
| 4.53 | 7.165(4) | 7.411(4) | 10.202(5) | 541.7 |
| 5.33 | 7.088(5) | 7.389(5) | 10.174(6) | 532.8 |
| 6.04 | 7.021(4) | 7.362(4) | 10.162(5) | 525.3 |
| 6.94 | 6.965(4) | 7.335(5) | 10.134(6) | 517.7 |

Estimated standard deviations are in brackets.

More information on the high-pressure behaviour of $CsMgInF_6$ was obtained from single-crystal X-ray diffraction. An inspection of reciprocal space sections reconstructed from data sets at different pressures also revealed splitting of reflections. Indexing always yielded a primitive orthorhombic lattice. Although reflections violating the body-centered lattice are very weak, a small number of them could be reliably observed. Taking into account the twinning model described in [2], the data are in accordance with space group *Pnma* at all pressures. This observation indicates that $CsMgInF_6$ does not undergo any structural phase transformation up to at least 6.94 GPa.

The pressure dependence of the lattice parameters and unit-cell volumes obtained from single-crystal X-ray data (Table 1) is presented in Fig. 3. $CsMgInF_6$ is the most and the least compressible along the $a$ and $b$ axes, respectively. The $P$–$V$ data could be fitted by a Birch–Murnaghan equation of state[3] with the zero-pressure bulk modulus $B_0 = 33.4(3)$ GPa and the unit-cell volume at ambient pressure $V_0 = 603.2(4)$ Å$^3$ for the first pressure derivative of the bulk modulus $B' = 4.00$.

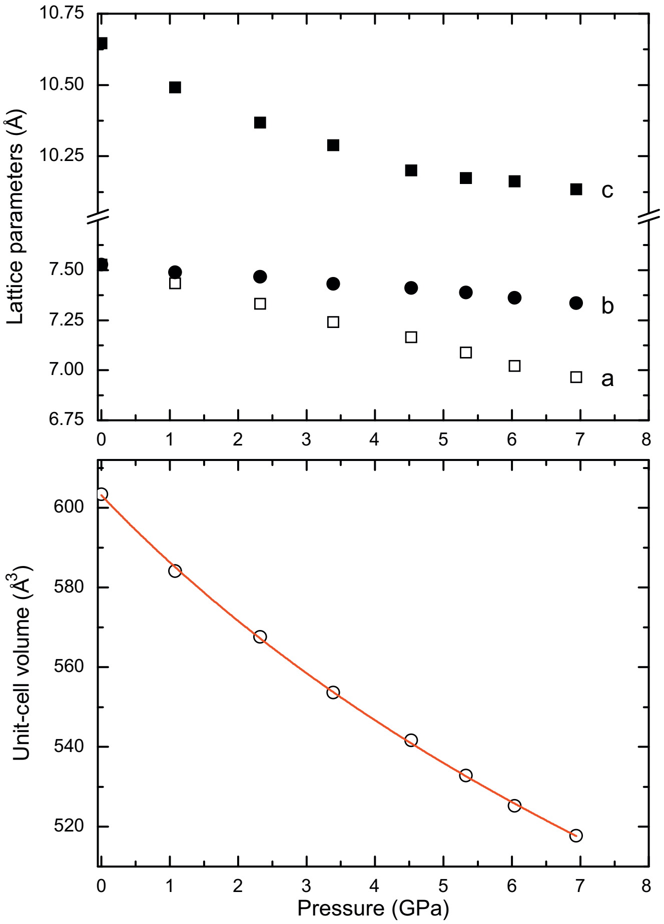

**Fig. 3.** Pressure dependence of the lattice parameters and unit-cell volume. The solid line represents the fit to the compressibility data using the Birch–Murnaghan equation of state: $V_0 = 603.2(4)$ Å$^3$, $B_0 = 33.4(3)$ GPa, and $B' = 4.00$.

---

[3] Program EoS-Fit V5.2 by Ross Angel, www.crystal.vt.edu/crystal/software.html

**Table 2**
Experimental data for the measurements at 6.04 GPa (*Pnma*, $Z = 4$).

| | |
|---|---|
| *Crystal data* | |
| $a$ (Å) | 7.021(4) |
| $b$ (Å) | 7.362(4) |
| $c$ (Å) | 10.162(5) |
| $V$ (Å$^3$) | 525.3 |
| $\rho$ (g/cm$^3$) | 4.880 |
| $\mu$ (mm$^{-1}$) | 11.487 |
| *Data collection* | |
| No. measured refl. | 2731 |
| Range of $h\,k\,l$ | $-8 \le h \le 7$<br>$-7 \le k \le 8$<br>$-11 \le l \le 11$ |
| No. unique refl. | 512 |
| No. observed refl.[a] | 119 |
| $R(\mathrm{int})_{\mathrm{obs/all}}$[b] | 10.19/15.52 |
| $\sin(\theta)/\lambda$ | 0.6679 |
| *Refinement*[b] | |
| $R_{\mathrm{obs}}$ | 9.31 |
| $wR_{\mathrm{obs}}$ | 7.46 |
| $\mathrm{GoF}_{\mathrm{obs}}$ | 1.53 |
| No. parameters | 26 |

[a] Criterion for observed reflections is $|F_{\mathrm{obs}}| > 3\sigma$.

[b] All agreement factors are given in %, weighting scheme $1/[\sigma^2(F_{\mathrm{obs}}) + (0.01F_{\mathrm{obs}})^2]$.

**Table 3**
Positional and isotropic thermal displacement parameters (in Å$^2$) at 6.04 GPa (*Pnma*, $Z = 4$).

| Atom | W.P. | $x$ | $y$ | $z$ | $U_{\mathrm{iso}}$ | Occupancy |
|---|---|---|---|---|---|---|
| Cs | *4c* | 0.4767(13) | 0.25 | 0.3665(7) | 0.050(3) | 1.0 |
| In1/Mg1 | *4b* | 0.0 | 0.0 | 0.5 | 0.052(3) | 0.5/0.5 |
| In2/Mg2 | *4c* | 0.287(2) | 0.25 | 0.7156(14) | 0.051(4) | 0.5/0.5 |
| F1 | *8d* | 0.305(6) | 0.022(5) | 0.835(3) | 0.078(8) | 1.0 |
| F2 | *8d* | 0.235(6) | 0.425(5) | 0.549(4) | 0.078(8) | 1.0 |
| F3 | *4c* | 0.365(8) | 0.25 | −0.008(5) | 0.078(8) | 1.0 |
| F4 | *4c* | 0.090(7) | 0.25 | 0.827(6) | 0.078(8) | 1.0 |

**Table 4**
Selected distances (Å) at 6.04 GPa.

| | |
|---|---|
| *Cs* | |
| F1 (2$x$) | 2.84(4) |
| F1 (2$x$) | 3.25(4) |
| F1 (2$x$) | 4.17(4) |
| F2 (2$x$) | 2.82(4) |
| F2 (2$x$) | 3.25(4) |
| F2 (2$x$) | 4.29(4) |
| F2 (2$x$) | 4.77(4) |
| F3 | 3.08(5) |
| F3 | 3.89(5) |
| F3 | 4.53(5) |
| F3 (2$x$) | 4.57(3) |
| F4 | 3.21(6) |
| F4 (2$x$) | 3.73(1) |
| *In1, Mg1* | |
| F1 (2$x$) | 2.17(4) |
| F2 (2$x$) | 1.81(4) |
| F3 (2$x$) | 2.07(2) |
| *In2, Mg2* | |
| F1 (2$x$) | 2.07(4) |
| F2 (2$x$) | 2.16(4) |
| F4 | 1.79(6) |
| F4 | 2.17(5) |

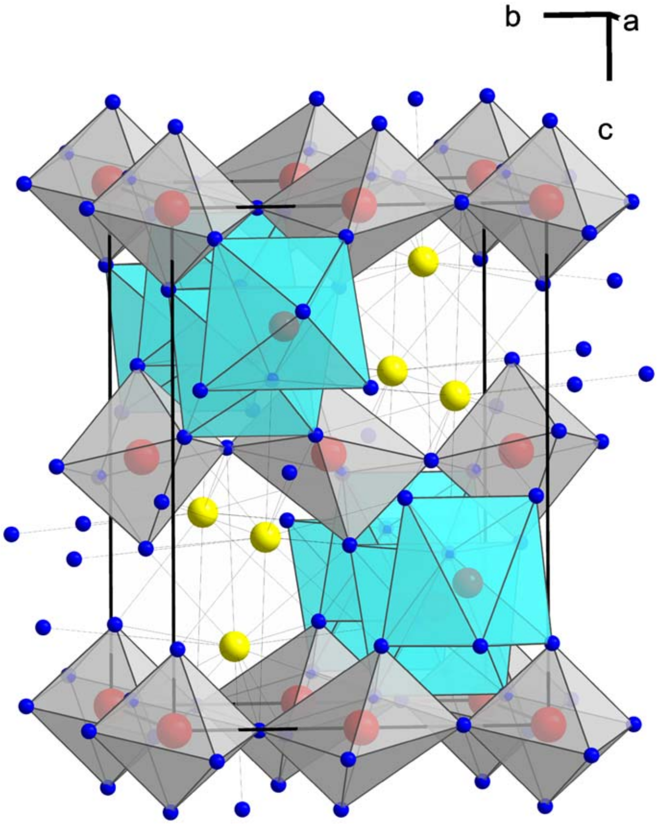

**Fig. 4.** Crystal structure of CsMgInF$_6$ (*Pnma*, $Z = 4$) at 6.04 GPa. Yellow, red, and blue symbols represent the Cs, (Mg/In), and F atoms, respectively. Octahedra around the (In1/Mg1) and (In2/Mg2) atoms are drawn grey and cyan, respectively. (For interpretation of the references to colour in this figure legend, the reader is referred to the web version of this article.)

The structural refinement of the data set at 6.04 GPa was performed with the program Jana2006 [9] (Table 2). The starting model in space group *Pnma* ($Z = 4$) was derived from the ideal pyrochlore structure ($Fd\bar{3}m$, $Z = 4$) using group–subgroup relations for splitting of Wyckoff positions (program WYCKSPLIT [10]).[4] Initially, the fluorine atoms were fixed at the ideal position derived from the cubic archetype and only the heavy atoms were refined. In subsequent refinement cycles, the symmetry restrictions on the positional parameters of the anionic sublattice were eliminated. The refinement of the occupancy factors of the In and Mg atoms did not indicate any onset of additional ordering. The final refinement (Table 3) included the positional parameters for all atoms, with the occupancies for the two *B* sites maintained at 0.5 In+0.5 Mg. Isotropic thermal parameters were refined for the In/Mg sites. All isotropic displacement parameters for the F atoms were restricted to be equal. The displacement parameter for the Cs atoms, the heaviest in the structure, was refined anisotropically.

Due to the twinning [2], some of the reflections were fully or partially overlapped. They were included in the refinement process allowing for a maximum angular difference of 0.2° for the overlap. The twinning matrices used in the refinements were

$$\begin{pmatrix} 1 & 0 & 0 \\ 0 & 1 & 0 \\ 0 & 0 & 1 \end{pmatrix}, \quad \begin{pmatrix} -0.5 & -0.5 & 1 \\ 0.5 & 0.5 & 1 \\ -0.5 & 0.5 & 0 \end{pmatrix}, \quad \begin{pmatrix} -0.5 & 0.5 & -1 \\ -0.5 & 0.5 & 1 \\ 0.5 & 0.5 & 0 \end{pmatrix},$$

---

[4] Bilbao Crystallographic Server, www.cryst.ehu.es

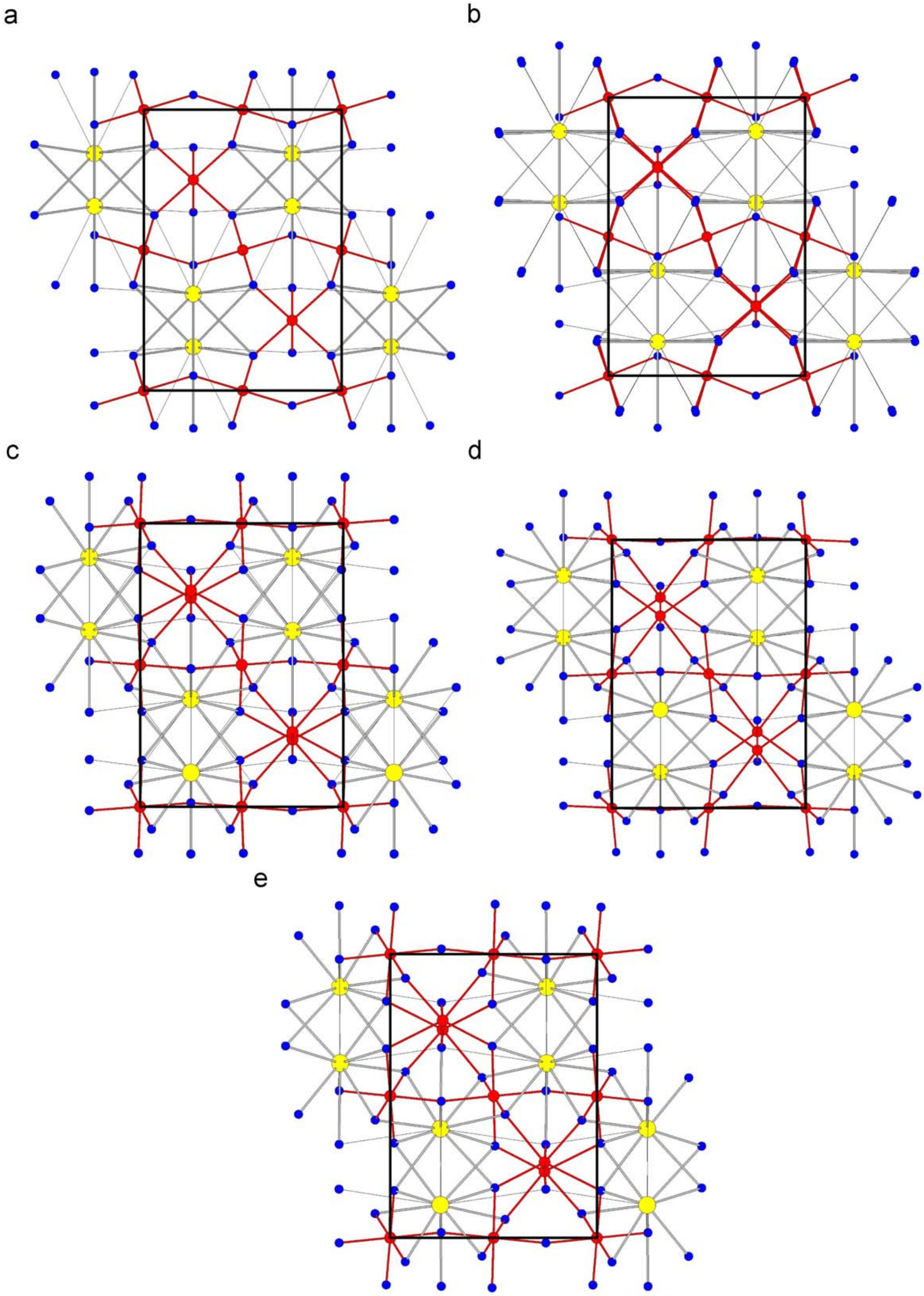

**Fig. 5.** Cation–fluorine connectivities in the crystal structures of $CsCu^{2+}Cu^{3+}F_6$ (*Imma*, $Z = 4$) (a), $CsMgInF_6$ (*Pnma*, $Z = 4$) (b), $KCuAlF_6$ (*Pnma*, $Z = 4$) (c), $CsMgInF_6$ at 6.04 GPa (*Pnma*, $Z = 4$) (d), and $KCuCrF_6$ ($P2_1/c$, $Z = 4$) (e). Except for (d), all the other figures depict the connectivities at ambient pressure. The projections for figures (a)–(d) and (e) are (*b*, *c*) and (*a*, *c*), respectively. Yellow, red, and blue symbols represent the *A*, *B*, and F atoms, respectively. The interatomic distances between the *B* atoms and fluorines below 2.5 Å are drawn red. The interatomic distances between the *A* atoms and fluorines up to 3.5 Å and from 3.5 to 4 Å are drawn as thick and thin lines, respectively. (For interpretation of the references to colour in this figure legend, the reader is referred to the web version of this article.)

$$\begin{pmatrix} 0 & 1 & 0 \\ -1 & 0 & 0 \\ 0 & 0 & 1 \end{pmatrix}, \begin{pmatrix} 0.5 & -0.5 & 1 \\ -0.5 & 0.5 & 1 \\ -0.5 & -0.5 & 0 \end{pmatrix} \text{ and } \begin{pmatrix} -0.5 & -0.5 & -1 \\ -0.5 & -0.5 & 1 \\ -0.5 & 0.5 & 0 \end{pmatrix}.$$

The refinement of the twin volume fractions lead to a considerable improvement of the overall agreement factors. The fractions are 0.56(2): 0.0: 0.10(2): 0.11(2): 0.17(2): 0.06(2).

The crystal structure of $CsMgInF_6$ at 6.04 GPa (Table 4 and Fig. 4) is largely distorted in comparison to that at ambient pressure. The major contribution to the bulk compressibility arises from the coordination changes around the Cs atoms. Assuming the limiting distance of 4 Å for the Cs–F interatomic distances, the coordination number of the Cs atoms is 13 (Table 3), while it is 18 at ambient pressure [2]. Four of the distances are below 2.9 Å and are shortened by approximately 13% when compared to the ambient pressure values. The anisotropic compressibilies could well be explained with different pressure-induced changes around the Cs atoms along three crystallographic directions. The largest changes in bonding occur along the *a* axis so that they account for the fact that the *a* linear compressibility is the largest.

Like in all other fluorides, the bulk modulus of $CsMgInF_6$, $B_0 = 33.4(3)$ GPa, is very small when compared with those of analogous oxides [3,11]. On the other hand, it is also much smaller than those of $NaCaMg_2F_7$ and $NaCdZn_2F_7$ pyrochlores, $B_0 \approx 83$ GPa, because of the large compressibility of the Cs coordination sphere.

The behaviour of the octahedra around the cations at the *B* sites in $CsMgInF_6$ reflects the mixed occupancies. Like in the $InF_6$ octahedra in $Li_3Na_2In_2F_{12}$ [11], the edge-length and angular distortions of the $(In1/Mg1)F_6$ and $(In2/Mg2)F_6$ octahedra increase on compression (Fig. 4). On the other hand, the shortest (In1/Mg1)–F and (In2/Mg2)–F interatomic distances (Table 3) compare well with the Mg–F distances in $NaCaMg_2F_7$ pyrochlore at high pressures [3].

The distortion of the high-pressure structure could be quantified by analysing its pseudosymmetry (program PSEUDO [12])[4] with respect to space group *Imma* that is a minimal supergroup of *Pnma* (Figs. 1 and 5). The atomic displacements necessary to obtain a structure with symmetry *Imma* are below 0.15 Å for all atoms at ambient pressure [2]. They increase substantially on compression and are 0.322, 0.865, 1.273, 1.896, and 1.250 Å for the Cs, In2/Mg2, F1/F2, F3, and F4 atoms, respectively, at 6.04 GPa.[5] It is noteworthy that these values are similar to the ones observed in other fluoride pyrochlores with symmetry *Pnma* ($Z = 4$) at ambient conditions, e.g., $KCuAlF_6$ (K: 0.184 Å, Cu: 0.823 Å, F1/F2: 1.216 Å, F3: 0.864 Å, F4: 0.898 Å, [13]).

Fig. 5 shows projections of selected defect pyrochlores with different degrees of distortions. As can be seen in Figs. 5a [13] and b [2], the distortions in $CsMgInF_6$ at ambient conditions with respect to the *Imma* structure are indeed minimal, with the six nearest fluorine atoms around the $Cs^{1+}$ cation at distances below 3.5 Å forming a slightly deformed octahedron. Ordered $KCuAlF_6$ [13] is significantly more deformed (Fig. 5c). It is remarkable that the coordination spheres around the $Cs^{1+}$ and the $K^{1+}$ cations in the structures of $CsMgInF_6$ at 6.04 GPa (Fig. 5d) and of $KCuAlF_6$ (Fig. 5c), respectively, include nine nearest fluorine neighbours below 3.5 Å. On the other hand, the deviation of the In2/Mg2 atoms from the position 0.25, 0.25, and 0.75 (the ideal position in *Imma*) is more pronounced in $CsMgInF_6$ than that of the corresponding atom in $KCuAlF_6$ so that the strong distortions of the $(In2/Mg2)F_6$ octahedra are noticeable. Figs. 5a–d clearly demonstrate that the effect of hydrostatic pressure on $CsMgInF_6$ is comparable to the effect of chemical pressure exerted through the incorporation of ions of different sizes into the *A* and *B* sites in $AB^{2+}B'^{3+}F_6$ pyrochlores. The high-pressure structure of $CsMgInF_6$ also indicates that the degree of distortion of the pyrochlore structure can even be higher than what is observed in the related compounds at $P = 0.0001$ GPa. In this context it is interesting to consider the only monoclinic compound of the family, $KCuCrF_6$ (Fig. 5e, [14]). The structure of this material is very similar to the structure of $KCuAlF_6$, the main difference being a slightly larger inclination of the $BF_6$ octahedra with respect to the *c* axis and a more asymmetric coordination sphere around the $K^{1+}$ ion. It is thus remarkable that the pyrochlore structure, once it has reached a certain degree of deviation from the higher symmetric *Imma* structure, seems to follow two distinct paths to accommodate further distortions, one that is reflected in the high-pressure structure of disordered $CsMgInF_6$ and another that is occurring in ordered $KCuCrF_6$ at ambient pressure.

## 4. Conclusions

No ordering of the $In^{3+}$ and $Mg^{2+}$ cations is observed in $CsMgInF_6$ on compression to at least 6.94 GPa. The major contribution to the bulk compressibility arises from the changes in the coordination sphere around the Cs atoms. The effect of hydrostatic pressure on the crystal structure of $CsMgInF_6$ is comparable to the effect of chemical pressure owing to the incorporation of ions of different sizes into the *A* and *B* sites in defect $AB^{2+}B'^{3+}F_6$ pyrochlores.

## Acknowledgments

A.G. and K.F. acknowledge the Universidad del País Vasco, the Gobierno Vasco, and the Ministerio de Ciencia e Innovación for supporting their high-pressure laboratory.

## Appendix A. Supplementary material

Supplementary data associated with this article can be found in the online version at 10.1016/j.jssc.2009.04.026.

## References

[1] Inorganic Crystal Structure Database, Fachinformationszentrum Karlsruhe, Germany.
[2] K. Friese, J.-Y. Gesland, A. Grzechnik, Z. Kristallogr. 220 (2005) 614.
[3] A. Grzechnik, J.M. Posse, W. Morgenroth, K. Friese, J. Solid State Chem. 180 (2007) 1998.
[4] [a] G.J. Piermarini, S. Block, J.D. Barnett, R.A. Forman, J. Appl. Phys. 46 (1975) 2774;
[b] H.K. Mao, J. Xu, P.M. Bell, J. Geophys. Res. 91 (1986) 4673.
[5] A.P. Hammersley, S.O. Svensson, M. Hanfland, A.N. Fitch, D. Häusermann, High Pressure Res. 14 (1996) 235.
[6] R.J. Angel, J. Phys. Condens. Matter 5 (1993) L141.
[7] STOE & Cie GmbH, Darmstadt.
[8] R.J. Angel, J. Appl. Cryst. 37 (2004) 486.
[9] V. Petricek, M. Dusek, L. Palatinus, in: Jana2006, The Crystallographic Computing System, Institute of Physics, Praha, Czech Republic.
[10] E. Kroumova, J.M. Pérez-Mato, M.I. Aroyo, J. Appl. Cryst. 31 (1998) 646.
[11] A. Grzechnik, T. Balic-Zunic, E. Makovicky, J.-Y. Gesland, K. Friese, J. Phys. Condens. Matter 2915 (2006).
[12] E. Kroumova, M.I. Aroyo, J.M. Pérez-Mato, J.M. Igartua, S. Ivantchev, Acta Crystallogr. A 56 (Suppl) (2000) 144.
[13] G. Wingfeld, R. Hoppe, Z. Anorg. Allg. Chem. 516 (1984) 223.
[14] D. Kissel, R. Hoppe, Z. Anorg. Allg. Chem. 557 (1988) 161.

---

[5] The displacement of the In1/Mg1 atoms is zero.